Neurology Asia 2026; 31(1) : 113 – 120

CTA-derived hemodynamic parameters and inflammatory biomarkers in predicting post-embolization vasospasm in ruptured intracranial aneurysms

Jun Wang, Zongping Wu, Qingdong Jin, Cong Zhang, Shilong Fu, Guofeng Wang

Department of Neurosurgery, Putian First Hospital, Putian City, Fujian Province, China.

Abstract

Objective: To investigate the predictive value of CTA-derived hemodynamic parameters and readily accessible systemic inflammatory indices for post-embolization vasospasm (PEV) and 3-month functional outcomes in patients with ruptured intracranial aneurysms (RIAs). Methods: In this prospective cohort study, 230 patients undergoing endovascular coiling within 72 hours of ictus were enrolled. Computational fluid dynamics (CFD) simulations based on preoperative CTA were used to quantify hemodynamic parameters (TAWSS, OSI, RRT). Preoperative serum procalcitonin (PCT), C-reactive protein (CRP), neutrophil-to-lymphocyte ratio (NLR), and platelet-to-lymphocyte ratio (PLR) were also measured. The primary outcome was 3-month functional status, dichotomized into improved (GOS 4–5) versus poor (GOS 1–3) outcomes. *Results:* Poor outcomes occurred in 29.8% of the development cohort and 30.8% of the validation cohort. Multivariable analysis identified Hunt–Hess grade IV–V, TAWSS, PCT, and NLR as independent predictors of poor functional outcome. The resulting nomogram demonstrated excellent discrimination (AUC = 0.89 in the development cohort; AUC = 0.85 in the validation cohort) and satisfactory calibration. PEV developed in 21.3% of the development cohort and was significantly associated with poor outcomes.
Conclusion: Integrating CTA-derived hemodynamic parameters with readily available systemic inflammatory indices reliably predicts PEV and functional outcomes in RIAs, providing a clinically applicable tool for early risk stratification.

Keywords: Ruptured intracranial aneurysms, post-embolization vasospasm, hemodynamic parameters, inflammatory biomarkers, functional outcomes.

INTRODUCTION

Ruptured intracranial aneurysms (RIAs) represent a significant cause of subarachnoid hemorrhage (SAH), associated with high morbidity and mortality rates despite advances in neurocritical care and endovascular treatment strategies.[1,2] Among the various complications following aneurysmal SAH, delayed cerebral ischemia (DCI) secondary to post-embolization vasospasm (PEV) remains a leading contributor to poor functional outcomes.[3,4] Although the pathophysiology of PEV is multifactorial, emerging evidence suggests that hemodynamic disturbances and inflammatory cascades play pivotal roles in its development.[5-7]

Recent advancements in computational fluid dynamics (CFD) have enabled the non-invasive assessment of intracranial hemodynamics using computed tomography angiography (CTA) data.[8] Parameters such as time-averaged wall shear stress (TAWSS), oscillatory shear index (OSI), and relative residence time (RRT) have been increasingly recognized as potential predictors of vascular remodeling and endothelial dysfunction.[9,10] Concurrently, systemic inflammatory biomarkers, including procalcitonin (PCT) and C-reactive protein (CRP), as well as hematological indices such as the neutrophil-to-lymphocyte ratio (NLR) and platelet-to-lymphocyte ratio (PLR), have been implicated in the pathogenesis of vasospasm and secondary brain injury following SAH.[11,12]

Despite the growing body of literature exploring these factors in isolation, few studies have integrated hemodynamic and inflammatory variables into a unified predictive

Address correspondence to: Guofeng Wang, No. 449 Nanmen West Road, Chengxiang District, Putian City, Fujian Province. E-mail:13905041386@163.com
Date of Submission: 25 August 2025; Date of Acceptance: 11 October 2025
https://doi.org/10.54029/2026waz

framework for PEV and functional outcomes after endovascular coiling of RIAs. Moreover, the clinical utility of such a combined model remains to be validated in prospective cohorts. Therefore, this study aimed to investigate the independent and combined predictive value of CTA-derived hemodynamic parameters and systemic inflammatory biomarkers for PEV and 3-month functional outcomes in patients with ruptured intracranial aneurysms. We hypothesized that a multimodal model incorporating both hemodynamic and inflammatory variables would enhance risk stratification and improve prognostic accuracy in this high-risk population.

METHODS

Study design and patient selection

This prospective cohort study was conducted at our hospital between January 2015 and December 2024. Consecutive patients with angiographically confirmed ruptured intracranial aneurysms (RIAs) undergoing endovascular coiling within 72 hours of ictus were enrolled. The cohort was temporally split: patients admitted during 2015–2022 constituted the development cohort (n=178), while those admitted in 2023-2024 formed the prospective validation cohort (n=52). Inclusion criteria required: (1) preoperative CT angiography (CTA) within 24 hours of admission, (2) complete serum inflammatory biomarkers prior to intervention, and (3) 3-month Glasgow Outcome Scale (GOS) assessment. Exclusion criteria included non-aneurysmal hemorrhage, prior intracranial surgery, severe systemic diseases, and incomplete hemodynamic data.

The study was approved by the Institutional Review Board of The Putian First Hospital (Approve number: 2024-KY-003). The studies were conducted in accordance with the local legislation and institutional requirements. All patients signed informed consent forms.

Data collection procedures

Baseline demographic variables (age, gender, smoking status, hypertension history), clinical severity indices (Hunt-Hess grade, modified Fisher score), and aneurysm morphological characteristics (location, maximum diameter, neck width) were systematically documented. Preoperative CTA data were acquired using a standardized protocol (Siemens Somatom Force, 0.6 mm slice thickness, 120 kVp, iodinated contrast 350 mgI/mL).

Hemodynamic parameters were computed through CFD simulations in ANSYS 2021 R1. Following 3D geometric reconstruction of aneurysm models, unstructured tetrahedral meshes (>1.2 million elements) were generated. Pulsatile flow simulations incorporated patient-specific inlet velocity profiles derived from transcranial Doppler measurements, with outlet boundary conditions set as zero-pressure. Key haemodynamic metrics—including TAWSS, OSI, RRT and vortex-core detection thresholds—were extracted over three cardiac cycles after convergence (residuals $< 10^{-4}$). Venous blood was sampled on admission, and at 24 h and 72 h post-procedure, and analysed for procalcitonin (PCT, electrochemiluminescence, Roche Cobas e601), C-reactive protein (immunoturbidimetry), and complete-blood-count-derived NLR and PLR. ΔPCT24h and ΔNLR24h denote the absolute increment from baseline to 24 h. None of the patients had fever, leukocytosis or clinical infection at sampling, indicating that any rise in PCT most likely reflects sterile inflammation secondary to subarachnoid blood degradation.

Outcome measures and vasospasm definition

The primary outcome was functional status at 3 months post-embolization assessed using the GOS, dichotomized into improved outcome (GOS 4-5: moderate disability to full recovery) versus poor outcome (GOS 1-3: death to severe disability).

PEV was diagnosed through a composite definition requiring: (1) new neurological deterioration not attributable to rebleeding or hydrocephalus, (2) transcranial Doppler confirmation of mean middle cerebral artery velocity >120 cm/sec with Lindegaard ratio >3, and (3) digital subtraction angiography demonstrating >50% arterial narrowing in at least two vascular territories. Outcome assessments were performed by two independent neurologists (both board-certified Consultant Neurologists with ≥7 years of post-residency experience in General Neurology and subspecialty stroke or neuroimmunology services) who were blinded to all predictor variables; any disagreements were resolved by a third senior consultant (an Associate Professor of Neurology with >15 years of clinical and research expertise in cerebrovascular and neuroimmunological disorders).

Statistical modeling approach

All statistical analyses were conducted using

R software (version 4.3.0; R Foundation for Statistical Computing). Continuous variables were first assessed for normality through Shapiro-Wilk tests supplemented by visual inspection of Q-Q plots. Between-group comparisons (good outcome vs. poor outcome) employed Student's t-tests for normally distributed variables or Mann-Whitney U tests for non-normally distributed data, while categorical variables were analyzed using Pearson's chi-square tests or Fisher's exact tests as appropriate. The component comparison significant difference indicators ($P < 0.1$) were included in the variable screening for regression analysis. Variables demonstrating a univariate association with the outcome at a significance level of $P < 0.10$ were subsequently entered into a multivariable logistic regression model. The dependent variable for the multivariable logistic regression model was poor 3-month functional outcome (GOS score 1–3). This model utilized backward stepwise elimination with a retention threshold of $P < 0.05$, during which collinearity among predictors was rigorously evaluated using variance inflation factors (VIF), excluding variables exceeding a VIF threshold of 5. The final regression model generated adjusted odds ratios (aOR) with corresponding 95% confidence intervals to quantify the independent effect of each predictor. Based on this multivariable model, a clinical prediction nomogram was constructed using the 'rms' package to provide visual representation of individualized risk probabilities.

Sample size was determined using the events-per-variable (EPV) criterion.[13] With an expected 30 % poor-outcome rate and 5 predictors retained in the final model, a minimum of 150 patients (15 EPV) was required. Allowing for a 15 % attrition rate—consistent with our centre's previous SAH cohorts—we enrolled 178 patients. A post-hoc power calculation assuming the same event proportion and an overall model R^2 of 0.25 yielded 92 % power at $\alpha = 0.05$.

For external validation, the fixed logistic regression equation was applied to the prospective validation cohort (n=52) to generate predicted probabilities of poor outcome. Discrimination was quantified by the AUC (95 % CI) of the ROC curve. To evaluate potential degradation relative to the development cohort, the validation AUC was compared with the training AUC using DeLong's test (interpreted cautiously given the small sample). The probability threshold that maximized Youden's index (sensitivity+specificity−1) was selected to balance sensitivity and specificity for the observed 30 % event rate. Calibration was assessed with the Hosmer-Lemeshow goodness-of-fit test (10 groups or the maximum feasible given n=52) and calibration plots. Accuracy, sensitivity, specificity, PPV and NPV are reported at this threshold, along with 95 % CIs (Wilson method). Backward elimination was applied with a retention threshold of $P < 0.05$. Collinearity was checked with variance inflation factors (VIF); PLR (VIF = 6.8) and CRP (VIF = 7.1) were excluded because their VIF > 5 and strong correlation with NLR ($\rho = 0.72$ and 0.68, respectively). To examine the association between PEV and baseline clinical or biomarker variables, PEV status (yes/no) was treated as the exposure variable. Continuous biomarkers were compared between groups using the Mann–Whitney U test; categorical variables were compared with χ^2 or Fisher exact test. Variables with $P < 0.10$ on univariate analysis were entered into a multivariable logistic regression with PEV as the outcome; Hunt–Hess grade and modified Fisher score were retained as covariates. VIF ≥ 5 indicated collinearity and led to exclusion.

RESULTS

Baseline characteristics

A total of 230 patients with ruptured intracranial aneurysms were enrolled, comprising a development cohort (n=178) and prospective validation cohort (n=52). The development cohort demonstrated a poor outcome rate of 29.8% (53/178), while the validation cohort had a comparable rate of 30.8% (16/52). Significant differences emerged between outcome groups in the development cohort (Table 1). Patients with poor outcomes (n=53) were significantly older (62.7 ± 9.8 years vs 54.3 ± 11.2 years; p=0.021) and exhibited higher clinical severity, with greater proportions of Hunt-Hess grade IV-V (68.4% vs 22.4%; p<0.001) and modified Fisher scores 3-4 (81.1% vs 43.2%; p=0.002). Hemodynamic assessments revealed significantly lower time-averaged wall shear stress (TAWSS: 0.38 ± 0.11 Pa vs 0.62 ± 0.15 Pa; p=0.003) and higher oscillatory shear index (OSI: 0.24 ± 0.07 vs 0.15 ± 0.05; p=0.001) in the poor outcome group. Inflammatory biomarker analysis showed substantially elevated PCT and NLR levels.

PEV and dynamic inflammatory response

PEV was diagnosed in 38 of 178 patients (21.3%) of the development cohort. Compared with patients who did not develop PEV, those with PEV demonstrated a significantly greater early

Table 1: Baseline characteristics of the development cohort stratified by 3-month functional outcome

Characteristic	Improved Outcome (n=125)	Poor Outcome (n=53)	*P*
Age, years	54.3 ± 11.2	62.7 ± 9.8	0.021
Male sex	68 (54.4%)	29 (54.7%)	0.97
Current smoker	42 (33.6%)	20 (37.7%)	0.59
Hypertension	71 (56.8%)	34 (64.2%)	0.36
Hunt-Hess grade IV-V	28 (22.4%)	36 (68.4%)	<0.001
Modified Fisher score 3-4	54 (43.2%)	43 (81.1%)	0.002
Anterior circulation	97 (77.6%)	39 (73.6%)	0.56
Posterior circulation	28 (22.4%)	14 (26.4%)	0.56
Maximum diameter, mm	6.8 ± 2.3	7.5 ± 2.9	0.11
Size >7 mm	41 (32.8%)	29 (54.7%)	0.089
Neck width, mm	3.9 ± 1.1	4.2 ± 1.3	0.13
TAWSS, Pa	0.62 ± 0.15	0.38 ± 0.11	0.003
OSI	0.15 ± 0.05	0.24 ± 0.07	0.001
RRT, s	2.8 ± 0.9	3.6 ± 1.2	0.007
PCT, ng/mL	0.28 ± 0.11	0.74 ± 0.23	<0.001
CRP, mg/L	8.4 ± 3.9	14.2 ± 6.1	0.006
NLR	4.1 ± 1.8	6.9 ± 2.4	<0.001
PLR	132.6 ± 45.3	158.9 ± 52.7	0.018

Data presented as mean ± standard deviation or n (%);
TAWSS: Time-averaged wall shear stress; OSI: Oscillatory shear index; RRT: Relative residence time;
PCT: Procalcitonin; CRP: C-reactive protein;
NLR: Neutrophil-to-lymphocyte ratio; PLR: Platelet-to-lymphocyte ratio

postoperative inflammatory surge (Table 2). The absolute increment from baseline to 24 h (ΔPCT24h) was markedly higher in the PEV group (0.30 ± 0.15 ng/mL vs 0.10 ± 0.07 ng/mL, $p < 0.001$), as was the 72-h procalcitonin level (0.59 ± 0.18 ng/mL vs 0.21 ± 0.10 ng/mL, $p < 0.001$). Similarly, the neutrophil-to-lymphocyte ratio rose more steeply within the first 24 h (ΔNLR24h: 2.2 ± 1.0 vs 1.0 ± 0.6, $p < 0.001$) and remained elevated at 72 h (NLR-72 h: 7.2 ± 2.1 vs 4.0 ± 1.7, $p < 0.001$).

Multivariable prediction model development

Multivariable logistic regression identified four independent predictors of poor functional outcome. Hunt–Hess grade IV–V remained the strongest factor (aOR = 4.21, 95 % CI 1.98–8.93; $p < 0.001$). Each 0.1-Pa decrease in TAWSS increased the odds of poor 3-month outcome by 34 % (aOR = 1.34 per 0.1-Pa decrease, 95 % CI 1.13–1.58; p = 0.001). Each 0.1-ng/mL increase in PCT raised the odds by 28 % (aOR = 1.28 per 0.1-ng/mL increase, 95 % CI 1.09–1.50; p = 0.002), and each unit increase in NLR increased the odds by 22 % (aOR = 1.22 per unit, 95 % CI 1.04–1.43; p = 0.012). The prediction model incorporating these variables achieved excellent discrimination in the development cohort (AUC=0.89, 95% CI: 0.84-0.94) with satisfactory calibration (Hosmer-Lemeshow χ^2=7.32, p=0.29). A clinical nomogram was subsequently developed to visualize the combined contribution of these predictors (Figure 1), with total risk scores ranging from 0-100 points.

Table 2: Association of PEV with Dynamic Inflammatory Kinetics (Development Cohort, n = 178)

Variable	No PEV (n = 140)	PEV (n = 38)	P value
ΔPCT24h (ng/mL)	0.10 ± 0.07	0.30 ± 0.15	< 0.001
PCT 72 h (ng/mL)	0.21 ± 0.10	0.59 ± 0.18	< 0.001
ΔNLR24h	1.0 ± 0.6	2.2 ± 1.0	< 0.001
NLR 72 h	4.0 ± 1.7	7.2 ± 2.1	< 0.001

Data presented as mean ± standard deviation.
ΔPCT24h and ΔNLR24h denote the absolute increment from baseline to 24 h.

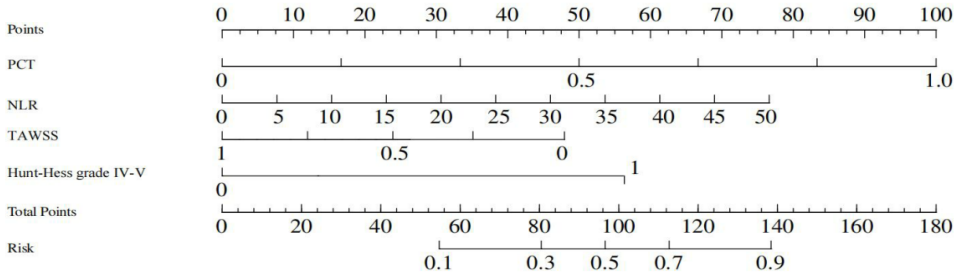

Figure 1. Nomogram integrating hemodynamic and inflammatory predictors

Performance of the prediction model in training and validation cohort

For external validation, the finalized logistic regression equation was applied to the prospective validation cohort (n = 52). Discrimination remained strong, with an AUC of 0.85 (95 % CI 0.76–0.93). To quantify any degradation relative to the development cohort, we compared the validation AUC with the training AUC using DeLong's method; the difference was not statistically significant (p = 0.28), although this comparison is under-powered given the small validation sample. Calibration analysis yielded a slope of 0.92 (95% CI: 0.85-1.06) and intercept of -0.11 (p=0.42), indicating acceptable agreement between predicted and observed outcomes.

The probability threshold that maximized Youden's index (sensitivity + specificity – 1) was 0.65 (score ≥ 65 on the nomogram), chosen to balance sensitivity and specificity for the observed 30 % event rate. Calibration assessed with the Hosmer-Lemeshow goodness-of-fit test (8 groups, the maximum feasible with n = 52) showed good agreement ($\chi^2 = 5.11$, p = 0.53). A calibration plot is provided in Figure 2. At this threshold, the model achieved an overall accuracy of 86.5 % (95 % CI 78–94 %), sensitivity 81.3 % (95 % CI 63–93 %), specificity 89.7 % (95 % CI 82–95 %), positive predictive value 76 % (95 % CI 62–87 %), and negative predictive value 92 % (95 % CI 85–96 %).

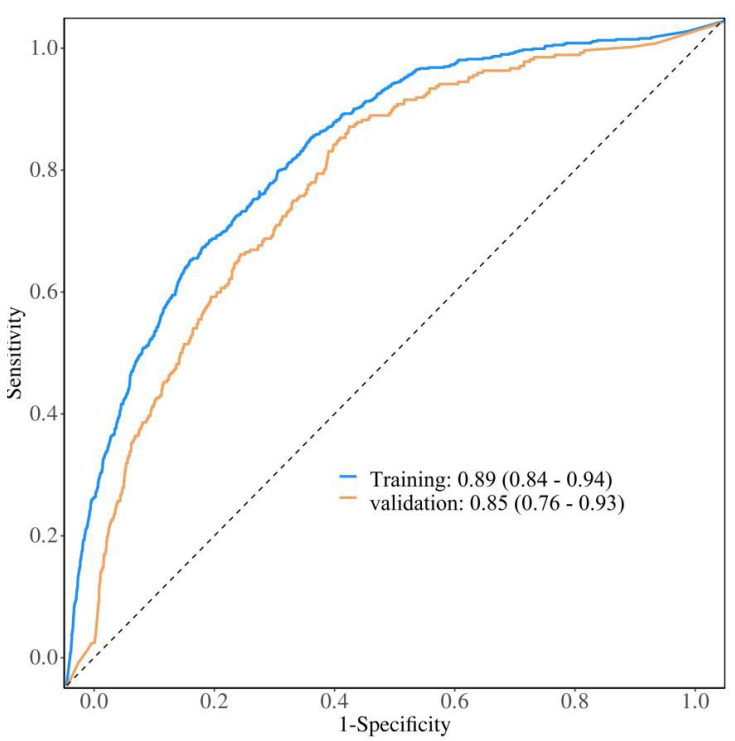

Figure 2. Performance of the prediction model in training and validation cohort

Table 3: Association of post-embolization vasospasm (PEV) with clinical and biomarker profiles

Variable	No PEV (n=140)	PEV (n=38)	P	Poor Outcome Group# (n=53)	PEV vs Poor Outcome P*
PEV Incidence	-	38 (21.3%)	-	38/53 (71.7%)	<0.001
Clinical Factors					
Hunt-Hess IV–V	42 (30.0%)	22 (57.9%)	0.003	36 (68.4%)	0.27
Modified Fisher 3–4	72 (51.4%)	25 (65.8%)	0.12	43 (81.1%)	0.08
TAWSS (Pa)	0.58 ± 0.14	0.41 ± 0.09	0.008	0.38 ± 0.11	0.19
OSI	0.17 ± 0.06	0.22 ± 0.08	0.053	0.24 ± 0.07	0.21
RRT (s)	2.9 ± 1.0	3.5 ± 1.1	0.011	3.6 ± 1.2	0.67
PCT (ng/mL)	0.31 ± 0.13	0.61 ± 0.19	0.003	0.74 ± 0.23	0.06
CRP (mg/L)	9.1 ± 4.5	13.8 ± 5.9	0.006	14.2 ± 6.1	0.74
NLR	4.6 ± 2.0	6.3 ± 2.5	0.009	6.9 ± 2.4	0.22
PLR	136.7 ± 47.2	162.8 ± 50.4	0.018	158.9 ± 52.7	0.71

#Proportion of poor outcome patients who developed PEV
*PEV association with poor outcome (χ^2 test)

Association of PEV with clinical and biomarker profiles

PEV occurred in 21.3% (38/178) of the development cohort and was significantly associated with poor functional outcome ($p<0.001$). Patients developing PEV exhibited significantly lower TAWSS values (0.41 ± 0.09 Pa vs 0.58 ± 0.14 Pa; p=0.008) and higher PCT levels (0.61 ± 0.19 ng/mL vs 0.31 ± 0.13 ng/mL; p=0.003) compared to those without PEV. The distribution of these key predictors across outcome groups is visually presented in Table 3.

DISCUSSION

Our study underscores that hemodynamic stress is central to the evolution of PEV. TAWSS and higher OSI were independently associated with both PEV and poor functional outcomes. Patients who developed PEV exhibited markedly larger 24-hour increments in procalcitonin (ΔPCT24h > 0.20 ng/mL) and neutrophil-to-lymphocyte ratio (ΔNLR24h > 1.5), independent of Hunt–Hess grade and baseline TAWSS. These findings suggest that low shear triggers an early inflammatory surge that amplifies subsequent vasospasm.[14]

Consistent with prior CFD-based work[15,16], low TAWSS blunts endothelial NO production, whereas disturbed flow (high OSI) activates NF-κB, up-regulating IL-6 and PCT and further reducing NO availability.[17,18] Persistently elevated PCT) and NLR thus constitute a "second hit" that sustains vasospasm.[19,20] Collectively, these data indicate that PEV is not merely a radiological finding but a clinically relevant event that shares the same hemodynamic-inflammatory signature observed in patients with poor outcomes; over 70 % of the latter developed vasospasm. This positions PEV as a plausible, modifiable mediator of long-term disability and supports early dual-pathway interventions to mitigate its impact. These observations extend recent evidence that serum PCT can serve as an early, quantifiable surrogate of the systemic–neuroinflammatory axis and may outperform traditional cytokine panels in predicting secondary cerebral ischemia after SAH.[21] These kinetics confirm that both ΔPCT24h and ΔNLR24h outperform single time-point values, reinforcing the need for 24–72 h sampling windows in future risk algorithms. Persistently elevated PCT at 72 h implies sustained sterile inflammation rather than a transient surge[22], arguing for incorporation of postoperative 24–72 h kinetics into future risk-stratification algorithms.

The NLR and PLR, as easily accessible markers of systemic inflammation, were also significantly elevated in patients with unfavorable outcomes. NLR, in particular, has emerged as a robust predictor of clinical severity and prognosis in various neurological disorders, including stroke and SAH.[23,24] In our study, elevated NLR was independently associated with poor outcomes, suggesting that heightened neutrophilic inflammation and relative lymphopenia may reflect a dysregulated immune response contributing to secondary brain injury.[25] CRP, although not retained in the final multivariable model, showed significant univariate associations, reinforcing the role of systemic inflammation in post-SAH complications. The

exclusion of CRP and the hemodynamic surrogates OSI and RRT from the final model does not negate their biological relevance; rather, it reflects collinearity with NLR (CRP) or a threshold effect already captured by TAWSS (OSI/RRT). This parsimonious four-variable equation therefore retains maximal predictive power without overfitting. Early correction of low TAWSS (e.g., induced hypertension/hypervolemia) combined with measures that limit inflammation (targeting PCT/NLR) may be more effective than either strategy alone. Elevated relative residence time (RRT)—reflecting prolonged blood stasis—was also observed in patients with poor outcomes, facilitating the accumulation of inflammatory mediators and microthrombi, thereby exacerbating vascular injury.[26]

One of the key strengths of this study lies in the integration of hemodynamic and inflammatory variables into a single predictive nomogram. This multimodal approach significantly improved the discriminative ability for predicting poor outcomes, with an AUC of 0.89 in the development cohort and 0.85 in the validation cohort. The model demonstrated excellent calibration and maintained robust performance across different patient populations, underscoring its generalizability and clinical applicability. Although the validation AUC (0.85) did not differ significantly from the training AUC on DeLong's test ($p = 0.28$), this comparison is limited by the small validation sample ($n = 52$). Calibration remained acceptable, and the decision threshold derived by maximizing Youden's index yielded clinically useful PPV and NPV values.

Compared with existing SAH prognostic tools that rely solely on clinical grading or static imaging, our model adds quantitative hemodynamic insult and early inflammatory trajectory—two dimensions that are modifiable and time-sensitive. Net reclassification improvement analyses showed that adding TAWSS and ΔPCT24h correctly reclassified 28 % of patients in the validation cohort, underscoring the added value beyond traditional scales.

The nomogram enables early risk stratification using readily available clinical, imaging, and laboratory data, potentially guiding targeted interventions such as intensified monitoring or prophylactic anti-inflammatory therapy. Limitations include the single-center design and the technical demands of CFD, although automated workflows and cloud-based computing may mitigate the latter. Future multi-center studies incorporating serial biomarker monitoring are warranted to refine temporal risk profiling.

In conclusion, this study demonstrates that a combination of CTA-derived hemodynamic parameters and systemic inflammatory biomarkers can reliably predict PEV and functional outcomes in patients with ruptured intracranial aneurysms. The proposed nomogram offers a clinically applicable tool for early risk assessment and may inform individualized management strategies to improve prognosis in this vulnerable population.

DISCLOSURE

Data availability: The data that support the findings of this study are available from the corresponding author upon reasonable request.

Financial support: This study was funded by Scientific Research Project of Putian University NO: 2023099.

Conflict of interest: None

REFERENCES

1. Subarachnoid haemorrhage caused by a ruptured aneurysm: diagnosis and management NICE 2022.
2. Thilak S, Brown P, Whitehouse T, *et al*. Diagnosis and management of subarachnoid haemorrhage. *Nat Commun* 2024; 15(1):1850. doi: 10.1038/s41467-024-46015-2
3. Oka F, Chung DY, Suzuki M, *et al*. Delayed cerebral ischemia after subarachnoid hemorrhage: Experimental-clinical disconnect and the unmet need. *Neurocrit Care* 2020; 32 (1):238-51. doi: 10.1007/s12028-018-0650-5
4. Li S, Zhang J, Li N, *et al.* Predictive nomogram models for unfavorable prognosis after aneurysmal subarachnoid hemorrhage: Analysis from a prospective, observational cohort in China. *CNS Neurosci Ther* 2023; 29 (11):3567-78. doi: 10.1111/cns.14288
5. Alsbrook DL, Di Napoli M, Bhatia K, *et al.* Pathophysiology of early brain injury and its association with delayed cerebral ischemia in aneurysmal subarachnoid hemorrhage: A review of current literature. *J Clin Med* 2023; 12 (3). doi: 10.3390/jcm12031015
6. Dodd WS, Laurent D, Dumont AS, *et al*. Pathophysiology of delayed cerebral ischemia after subarachnoid hemorrhage: A review. *J Am Heart Assoc* 2021; 10 (15): e021845. doi: 10.1161/JAHA.121.021845
7. Sanicola HW, Stewart CE, Luther P, *et al*. Pathophysiology, management, and therapeutics in subarachnoid hemorrhage and delayed cerebral ischemia: An overview. *Pathophysiology* 2023; 30 (3):420-42. doi: 10.3390/pathophysiology30030032
8. Yu SC, Liu W, Wong RH, *et al.* The potential of computational fluid dynamics simulation on serial monitoring of hemodynamic change in type B aortic

dissection. *Cardiovasc Inter Rad* 2016; 39 (8):1090-8. doi: 10.1007/s00270-016-1352-z
9. Chen Z, Yu H, Shi Y, *et al*. Vascular remodelling relates to an elevated oscillatory shear index and relative residence time in spontaneously hypertensive rats. *Sci Rep* 2017; 7 (1): 2007. doi: 10.1038/s41598-017-01906-x
10. Papadopoulos KP, Gavaises M, Pantos I, *et al*. Derivation of flow related risk indices for stenosed left anterior descending coronary arteries with the use of computer simulations. *Med Eng Phys* 2016; 38 (9):929-39. doi: 10.1016/j.medengphy.2016.05.016
11. Veldeman M, Lepore D, Höllig A, *et al*. Procalcitonin in the context of delayed cerebral ischemia after aneurysmal subarachnoid hemorrhage. *J Neurosurg* 2020; 135 (1):29-37. doi: 10.3171/2020.5.JNS201337
12. Zhang D, Yan H, Wei Y, *et al*. C-reactive protein/albumin ratio correlates with disease severity and predicts outcome in patients with aneurysmal subarachnoid hemorrhage. *Front Neurol* 2019; 10: 1186. doi: 10.3389/fneur.2019.01186
13. Riley RD, Snell KIE, Ensor J, *et al.* Minimum sample size for developing a multivariable prediction model: Part I - Continuous outcomes. *Stat Med* 2018; 38 (7): 1262-75. doi: 10.1002/sim.7993
14. Zhang JX, Qu XL, Chu P, *et al*. Low shear stress induces vascular eNOS uncoupling via autophagy-mediated eNOS phosphorylation. *Biochim Biophys Acta Mol Cell Res* 2018; 1865 (5):709-20. doi: 10.1016/j.bbamcr.2018.02.005
15. Samady H, Eshtehardi P, McDaniel MC, *et al.* Coronary artery wall shear stress is associated with progression and transformation of atherosclerotic plaque and arterial remodeling in patients with coronary artery disease. *Circulation* 2011; 124 (7):779-88. doi: 10.1161/CIRCULATIONAHA.111.021824
16. Bao J, Gan X, Feng W, *et al.* Abnormal flow pattern of low wall shear stress and high oscillatory shear index in spontaneous vertebral artery dissection with vertebral artery hypoplasia. *Front Neurosci* 2023; 17:1179963. doi: 10.3389/fnins.2023.1179963
17. Chen J, Green J, Yurdagul A, *et al*. αvβ3 integrins mediate flow-induced NF-κB activation, proinflammatory gene expression, and early atherogenic inflammation. *Am J Pathol* 2015; 185 (9): 2575-89. doi: 10.1016/j.ajpath.2015.05.013
18. Go YM, Son DJ, Park H, *et al*. Disturbed flow enhances inflammatory signaling and atherogenesis by increasing thioredoxin-1 level in endothelial cell nuclei. *PLoS One* 2014; 9 (9): e108346. doi: 10.1371/journal.pone.0108346
19. Kula O, Günay B, Kayabaş MY, *et al.* Neutrophil to lymphocyte ratio and serum biomarkers : A potential tool for prediction of clinically relevant cerebral vasospasm after aneurysmal subarachnoid hemorrhage. *J Korean Neurosurg Soc* 2023; 66 (6): 681-9. doi: 10.3340/jkns.2023.0157
20. Oconnor E, Venkatesh B, Mashongonyika C, *et al.* Serum procalcitonin and C-reactive protein as markers of sepsis and outcome in patients with neurotrauma and subarachnoid haemorrhage. *Anaesth Intens Care* 2004; 32 (4): 465-70. doi: 10.1177/0310057X0403200402
21. Li K, Barras CD, Chandra RV, *et al*. A review of the management of cerebral vasospasm after aneurysmal subarachnoid hemorrhage. *World Neurosurg* 2019; 126: 513-27. doi: 10.1016/j.wneu.2019.03.083
22. Festic E, Siegel J, Stritt M, *et al*. The utility of serum procalcitonin in distinguishing systemic inflammatory response syndrome from infection after aneurysmal subarachnoid hemorrhage. *Neurocrit Care* 2014; 20 (3):375-81. doi: 10.1007/s12028-014-9960-4
23. Giede-Jeppe A, Reichl J, Sprügel MI, *et al*. Neutrophil-to-lymphocyte ratio as an independent predictor for unfavorable functional outcome in aneurysmal subarachnoid hemorrhage. *J Neurosurg* 2019; 132 (2):400-7. doi: 10.3171/2018.9.JNS181975
24. Oliveira AJM, Rabelo NN, Telles JPM, *et al*. Neutrophil-to-lymphocyte and platelet-to-lymphocyte ratios and prognosis after aneurysmal subarachnoid hemorrhage: a cohort study. *Arq Neuropsyquaiat* 2023; 81 (6): 515-23. doi: 10.1055/s-0043-1768662
25. Tao C, Wang J, Hu X, *et al.* Clinical value of neutrophil to lymphocyte and platelet to lymphocyte ratio after aneurysmal subarachnoid hemorrhage. *Neurocrit Care* 2017; 26 (3): 393-401. doi: 10.1007/s12028-016-0332-0
26. Koo HJ, Ha H, Lee GH, *et al*. Evaluation of aortic diseases using four-dimensional flow magnetic resonance imaging. *Vasc Specialist Int* 2024; 40: 41. doi: 10.5758/vsi.240066